Minimum energy per bit in high bit rate optical communications and quantum communications

P. Gallion[a] and F. J. Mendieta[b]
[a] Telecom ParisTech,
Ecole Nationale Supérieure des Télécommunications and CNRS, LTCI
46, rue Barrault 75013 Paris, France
Email: gallion@enst.fr
[b] CICESE, Carretera Ensenada - Tijuana 3918, Fraccionamiento Zona Playitas
Ensenada, Baja California, 22860, Mexico
Email: mendieta@cicese.mx

Invited paper

ABSTRACT

Optical direct detection usually operates far above the quantum limit, due to the high thermal noise level of PIN photodiodes. For signal energy at the quantum level, the thermal effects in photon counters are also a strong limitation. The optical amplification or the heterodyne detection of the 2 quadratures of the field, widely used in high bit rate and long haul optical systems, overcome this limitation at the expense of a minimum 3db noise figure. By allowing a noise free mixing gain, as well as single quadrature measurements, the balanced homodyne receiver is allowed to reach quantum noise limited operation.

The aim of this paper is to review the different quantum receiver implementations and to compare the minimum signal energy required to achieve a given bit error rate, or a given bit erasure rate, in high bit rate communications and quantum communications. Application to quantum cryptography will be also addressed.

Keywords: Quantum receiver, Quantum noise, Homodyne detection, Quadrature measurements, Signal to noise ratio, Bit error rate, Quantum cryptography.

1. INTRODUCTION

Optical communications with low photon number signals constitutes an expanding field in a diversity of applications. In quantum cryptography applications, either in optical fibers[1,2,3,4,5,6], in free space[7], in aeronautic applications[8] and even in satellite systems[9], the information signals are, in general, prepared deliberately in low photon number for each transmitted symbol.

Furthermore, other non cryptographic applications requiring power economy frequently deal with these quantum level signals, such as quantum communications for airborne, space to ground and inter satellite scenarios. Diverse feasibility studies have been reported[1011,12] as well as proof of concept experiments have also been proposed[13,14,15,16].

Future optical communications systems beyond Earth orbits will have to operate very close to the ultimate quantum limits, and will rely not only on sensitive detectors but also on efficient modulation formats. Suppressed carrier constellations will be in general mandatory and (phase sensitive) receivers will be required for not only signal demodulation but also optical phase synchronization from the quantum level signals themselves These issues will be addressed in this work, and phase synchronization will be an important task especially in the section devoted to the experimental setups.

Other applications of low photon number detection are intensively researched at the telecommunications wavelengths, highly sensitive sensors[17], homodyne tomography[18], lidar systems and other instrumentation and scientific applications[19].

Preparation of quantum states for the different applications has been pursued since the first reports on the understanding of the fundamental limits, i.e. the Helström limit[20], and several proposals using non-classical states have been reported.

SPIE Eco-Photonics 2011: Sustainable Design, Manufacturing, and Engineering Workforce Education for a Green Future,
edited by Pierre Ambs, Dan Curticapean, Claus Emmelmann, Wolfgang Knapp, Zbigniew T. Kuznicki, Patrick P. Meyrueis,
Proc. of SPIE Vol. 8065, 80650F · © 2011 SPIE · CCC code: 0277-786X/11/$18 · doi: 10.1117/12.884781

However, quantum coherent states are the easiest to produce and receiver structures for optimal detection have been extensively studied and more recently implemented with photon counters and even photon number resolving detectors.

Our approach in this paper is to put in relevance the homodyne detection of weak coherent states signals, as an interesting alternative to the poor performances of photon counting techniques, given their characteristics inherited from the well developed optical networks field, related to their performances in speed and ease of integration with the existing fiber optic infrastructure and economics. For sake of simplicity we will avoid to use quantum mechanics formalism for which a description may be found in reference[21]. In the second part of the paper we first precise the notations used for the signal description and to the presentation of the various detection schemes using one, two or four detectors. The section 3 is devoted to On Off Keying (OOK) and polarization modulated signal receivers. The idealistic Kennedy and Dolinar single detector optical receivers for Binary Phase Shift Keyed (BPSK) signals are reviewed in section 4, after the recall of the PSK-modulated coherent states overlap and the Helström bound for their discrimination. In section 5, the 2-detectors balanced detection arrangement performances are presented. The double detector Kennedy receiver or double detector super homodyne receiver, based on the interference of the signal to be detected with a reference one of similar amplitude, requires the use of single photon counters. Emphasis is put on the double detector strong local oscillator homodyne receiver for BPSK signal, which can operate with low cost and high performance PIN photodiodes. In section 6 we report two experiments with balanced homodyne detection. A short conclusion ends the paper.

2. OPTICAL SIGNAL AND RECEIVER STRUCTURES

2.1 Signal normalization

In optical communication it is usual to deal with a quasi-monochromatic optical field $E(t)$ in a single spatial and polarization mode and with an angular central carrier frequency $\omega_0 = 2\pi\nu$, described by its complex slowly time-varying envelope $a(t)$ written as[21]

$$E(t) \propto \mathrm{Re}\left[\sqrt{\frac{h\nu}{T}}\,a(t)\exp j\omega_0 t\right] \tag{1}$$

where $\mathrm{Re}[\ ]$stands for the real part $[\ ]$. The time duration T refers to the observation time, which is the symbol duration in digital communication. T is simultaneously assumed to be as far longer than the optical period and as far smaller than the coherence duration of the optical source. The field envelope is so normalized that the short-time-average optical power P is given by

$$\langle P\rangle = h\nu\left\langle |a(t)|^2\right\rangle = \left\langle |E(t)|^2\right\rangle \tag{2}$$

where $h\nu$ is the photon energy and $h = 6.63.10^{-34}$ J.s is the Planck's constant.

In these conditions $|a(t)|$ is expressed as (number of photons)$^{1/2}$ and $|a(t)|^2$ is the signal energy, expressed as a number of photons, and *a(t)* will considered as the optical signal in the following.

2.2 Single detector direct detection receiver

In direct, or so-called incoherent detection, the photo detector device converts the photon flow into an electron flow as shown on Fig 1. The photo detector device is usually a PIN photodiode. The quantum efficiency of the detectors is assumed to be close the unity so that the output electron flow has the same value $N = aa^*$ than the input photon flow and also the same statistics.

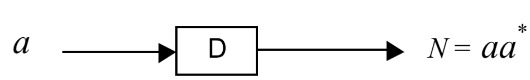

Figure 1: Basic direct detection arrangement

Expanding the detected field as in the sum of its 2 quadratures $a = a_I + ja_Q$, the output electron number is written as

$$N = a_I^2 + a_Q^2 \tag{3}$$

2.3 Balanced dual detector coherent receiver

- Receiver structure

The basic structure of a coherent receiver, displayed on Fig 2, is obtained by connection of 2 detectors D1 and D2 to each outputs of a balanced four-port optical coupler. The quantum efficiency of the 2 detectors is again assumed to be close the unity. The 2 detector outputs are therefore subtracted with a differential amplifier to produce the output electron number *N*.

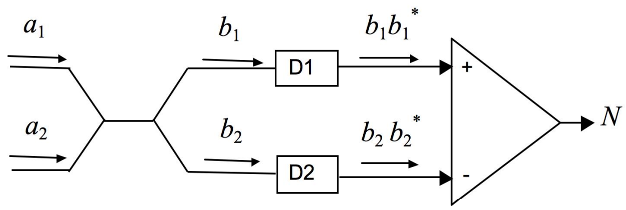

Figure 2: Balanced coherent receiver structure

Using the standard input to output relationship for the balanced optical coupler we have the output signals

$$\begin{pmatrix} b_1 \\ b_2 \end{pmatrix} = \frac{1}{\sqrt{2}} \begin{pmatrix} a_1 - ja_2 \\ a_2 - ja_1 \end{pmatrix} \tag{4}$$

According to the square law of the photo detectors their outputs are expressed as

$$N_1 = b_1 b_1^* = \frac{1}{2}\left[a_1 a_1^* + a_2 a_2^* + j(a_1 a_2^* - a_2 a_1^*)\right] \text{ and } N_2 = b_2 b_2^* = \frac{1}{2}\left[a_1 a_1^* + a_2 a_2^* - j(a_1 a_2^* - a_2 a_1^*)\right] \tag{5}$$

Assuming an unit-gain electrical amplifier with a gain equal to 1, the 2-output subtraction leads to the amplifier output

$$N = N_1 - N_2 = j(a_1 a_2^* - a_2 a_1^*) = -2\,\mathrm{Im}(a_1 a_2^*) \tag{6}$$

Expanding the 2 input signals a_1 and a_2 as the sum of their 2 quadratures

$$a_1 = a_{1I} + ja_{1Q} \quad \text{and} \quad a_2 = a_{2I} + \mathrm{j}a_{2Q} \tag{7}$$

The electron number at output of the amplifier may be written as

$$N = N_1 - N_2 = 2(a_{1I} a_{2Q} - a_{1Q} a_{2I}) \tag{8}$$

In a coherent receiver configuration the optical signal *s* to be detected is sent on one input and the local oscillator (LO) *l* is sent on the other in the form

$$a_1 = s \quad \text{and} \quad a_2 = jl \tag{9}$$

The additional phase shift expressed by the *j* factor in Eq. 9 is used to cancel the phase shift of the coupler for the LO on the detector D1. We have in this case a phase referencing on this detector for both the local and the signal and no more at the input of the coupler. Expanding the signal and the local fields may as the sum of their 2 quadratures, we finally obtain

$$N = 2\left(s_I l_I + s_Q l_Q\right) \tag{10}$$

The electron number appears as twice the scalar product of the signal and the local oscillator vectors. The coherent detection arrangement is a projection of the signal on the local field.

2.4 IQ four detector receiver

A more sophisticated receiver is the homodyne In-phase Quadrature receiver (IQ) using an eight-port hybrid coupler. As depicted by the Fig 3, it is the association of 4 2X2 couplers, a $\pi/2$ phase shifter and two balanced detection arrangements. Only the 2 input ports 1 and 2 are used for a mixing operation and it is easy to show that the scattering matrix of eight-port hybrid coupler my be written, in this case, as

$$\begin{pmatrix} b_1 \\ b_2 \\ b_3 \\ b_4 \end{pmatrix} = \frac{1}{2}\begin{pmatrix} 1 & -1 \\ -j & -j \\ -j & -1 \\ -1 & -j \end{pmatrix}\begin{pmatrix} a_1 \\ a_2 \end{pmatrix} = \frac{1}{2}\begin{pmatrix} a_1 - a_2 \\ -ja_1 - ja_2 \\ -ja_1 - a_2 \\ -a_1 - ja_2 \end{pmatrix} \tag{11}$$

The 4 detectors outputs are then given by

$$\begin{aligned} N_1 &= b_1 b_1^* = \frac{1}{4}\left[a_1 a_1^* + a_2 a_2^* - (a_1 a_2^* + a_2 a_1^*)\right] \qquad & N_2 &= b_2 b_2^* = \frac{1}{4}\left[a_1 a_1^* + a_2 a_2^* + (a_1 a_2^* + a_2 a_1^*)\right] \\ N_3 &= b_3 b_3^* = \frac{1}{4}\left[a_1 a_1^* + a_2 a_2^* + j(a_1 a_2^* - a_2 a_1^*)\right] \qquad & N_4 &= b_4 b_4^* = \frac{1}{4}\left[a_1 a_1^* + a_2 a_2^* - j(a_1 a_2^* - a_2 a_1^*)\right] \end{aligned} \tag{12}$$

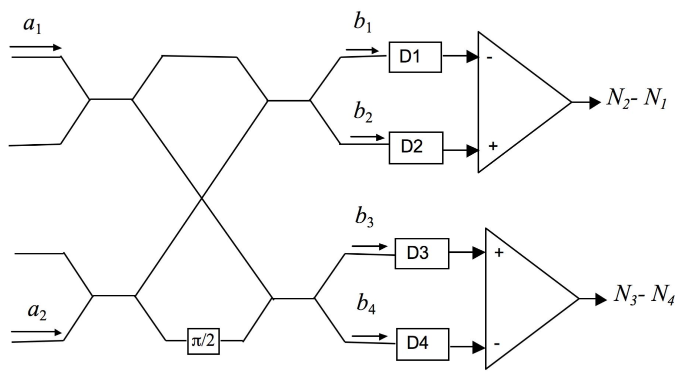

Figure 3: IQ 4-detector receiver

After 2 by 2 output subtractions we finally obtain

$$N_2 - N_1 = \mathrm{Re}(a_1 a_2^*) \quad \text{and} \quad N_3 - N_4 = \mathrm{Im}(a_1 a_2^*) \tag{13}$$

The real and imaginary parts of a_1 are obtained, a_2 acting as a phase reference. As for a heterodyne detection, the 2 quadratures of the field are simultaneously measured at the expense of a minimum 3db noise figure[22].

3. OOK AND POLARIZATION MODULATED SIGNAL RECEIVERS

3.1 Direct detection OOK receiver

Assuming that the average photon number during the bit “1” is N_1, and that the average photon number for the bit “0” is $N_0 = 0$, in an ideal on off keying (OOK) modulation situation with perfect extinction ratio, the average photon number per bit is $N_S = (N_1 + N_0)/2 = N_1/2$. Assuming also no thermal noise and other noises impairments, no noise at all is present when the symbol “0” is transmitted. The decision threshold is to set close to 0 and the probability *P(1/0)* to detect 1, when 0 is transmitted, is equal to zero. Errors only occur when the symbol “1” is transmitted and the corresponding probability of error *P(0/1)* is derived using the well-known conditional Poisson process at the detector. The probability *p(n)* to observe *n* photons when $\langle n \rangle$ are expected[23] is

$$p(n) = \frac{\langle n \rangle^n}{n!} \exp - \langle n \rangle \tag{14}$$

Errors occuring only when $n = 0$ is observed while $\langle n \rangle = N_1 = 2N_S$ is expected, and we have $P(0/1) = \exp(-2N_S)$. A binary message more informative for which the symbols "1" and "0" have the same probability to occur is assumed, so we have $p(1) = p(0) = 1/2$. The Bit Error Rate (BER) is thus given by

$$BErrorR = 1/2\left(P(0/1) + P(1/0)\right) \tag{15}$$

and the bit error rate of the direct detection receiver is

$$BErrorR = 1/2 \exp(-2N_S) \tag{16}$$

This detection situation is a degenerated since no errors are considered for the transmitted "0". It is not of great practical interest since this shot noise limited situation can unfortunately be only obtained for a high signal level or under low temperature operation when the associated shot noise overcomes the thermal noise. In this situation the average photon number per bit, required for a bit error rate equal to 10^{-9}, is

$$N_S = 10 \text{ photons/bit} \tag{17}$$

An equivalent situation is the detection of a signal switched between 2 orthogonal polarization states with a single detector following a polarizer. However, in this case, the useful average energy of the signal is divided by a 2 factor.

Due to the unavoidable thermal noise the number of required photons is usually dramatically larger, making direct detection inappropriate for low photon number signal detection. Due to its minimum noise factor $F = 2$, the utilization of an optical preamplifier to overcome the thermal noise leads to quantum limit of 38 photons/bit for OOK signals under matched filtering condition[23].

3.2 Two detector receiver for polarization modulated signal

Let us assume a polarization modulation encoding using 2 orthogonal eigenstates, using for instance the binary signal representations $|\rightarrow\rangle = |0\rangle$ and $|\uparrow\rangle = |1\rangle$. Since orthogonal polarization circular states refer to different quantum states they can, in principle, be error free discriminated.

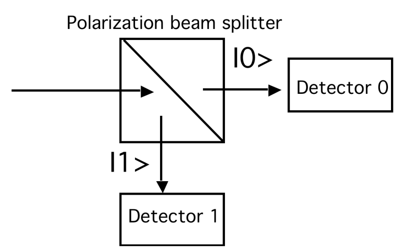

Figure 4: Linearly polarization switched signal receiver

As shown on Fig 4, the perfectly linearly polarized signal energy is not spread on the 2 detectors and the average photon number $N_S = N_1 = N_0$ is totally received by one of them. However, in the same way as for an OOK signal detection, no photon may be received when N_S are expected. In this case the probability of erasure of the receiver is derived using the well-known conditional Poisson process at the photon counter and the well-known probability *p(n)* to observe $n = 0$ photons while N_S is expected

$$BErassureR = \exp(-N_S) \tag{18}$$

In quantum cryptography applications this arrangement may by use for quantum key distribution, the erasure rate is not usually a major drawback since the corresponding information may be discarded during the reconciliation process, at the expense of a reduction of the key rate generation.

In digital communication the erasures, which are localized, may be corrected by using a forward error-coding (FEC) overhead. When no coding is used the erasure rate turns to a *BErrorRate* equal to the half of the erasure rate

$$BErrorR = 1/2\exp\left(-N_S\right) \tag{19}$$

According to Eq. 19, the average photon number $N_S = 20$ is required to achieve a bit error rate equal to 10^{-9}.

4. SINGLE DETECTOR OPTICAL RECEIVERS FOR PSK SIGNAL

4.1 PSK modulated coherent state overlap

Coherent states are the more classical-like signals and, up to now, the more widely used in optical communication and cryptography. They are easily produced by reliable and inexpensive semiconductor laser sources covering the larger part of the today's application fields. Furthermore, the excess noise of a nearly coherent state source disappears through attenuation, turning it into a coherent state.

However the error free discrimination of 2 coherent states is impossible since they are not orthogonal. The state overlap of 2 different coherent states is easily derived by using the non-orthogonal coherent states expansion as a sum of orthogonal number of photon number states

$$\left|\alpha\right\rangle = \exp(-\frac{1}{2}\left|\alpha\right|^2)\sum_{n=0}^{\infty}\frac{\alpha^n}{\sqrt{n!}}\left|n\right\rangle \tag{20}$$

The square of the components in this expansion is the well-known Poisson distribution.

$$\left|\left\langle\alpha_1\middle|\alpha_2\right\rangle\right|^2 = \left|\exp\left[-\frac{1}{2}(\left|\alpha_1\right|^2+\left|\alpha_2\right|^2)\right]\sum_{n=0}^{\infty}\sum_{m=0}^{\infty}\frac{\alpha^{*n}}{\sqrt{n!}}\frac{\alpha^m}{\sqrt{m!}}\left\langle n\middle|m\right\rangle\right|^2 = \exp(-\left|\alpha_1-\alpha_2\right|^2) \tag{21}$$

For binary phase-shift keying (BPSK) modulated coherent state signal, the two antipodal coherent states are $\left|\alpha\right\rangle$ and $\left|-\alpha\right\rangle$ are used to minimize their overlap for a given average signal photon number $N_s = \left|\alpha\right|^2$. The signal overlap is in this case

$$\left\langle\alpha\middle|-\alpha\right\rangle = \exp(-\left|2\alpha\right|^2) = \exp(-4N_S) \tag{22}$$

In the same way, for OOK signal, the overlap of the coherent state with the vacuum state is to be considered

$$\left\langle\alpha\middle|\alpha=0\right\rangle = \exp(-\left|\alpha\right|^2) = \exp(-N_S) \tag{23}$$

4.2 Helström Bound

Since a complete differentiation of the transmitted BPSK states is not possible, an inherently finite error rate is obtained. For non-orthogonal signal states, using the maximum likelihood criterion, Helström found the minimum attainable probability of error as a function of the signal state overlap $\left\langle\alpha_1\middle|\alpha_2\right\rangle$. Assuming an identical probability of transmission it is expresses in terms of the two states overlap

$$BErrorR = 1/2\left(1-\sqrt{1-\left\langle\alpha_1\middle|\alpha_2\right\rangle}\right) \tag{24}$$

Using the 2 coherent states overlap of a BPSK signal, the *BErrorRate* finally is expressed as

$$BErrorR = 1/2\left(1-\sqrt{1-\exp\left(-4N_S\right)}\right) \approx 1/4\exp\left(-4N_S\right) \tag{25}$$

4.3 Single detector Kennedy receiver or single detector super homodyne receiver

The Kennedy receiver performs the detection of BPSK signals using a single photo detector by adding a phase referenced local oscillator with the same amplitude, supposed already known, on the receiver[24,25]. The added local oscillator corresponds to one of the 2 possible realizations for the signal, which is then doubled, and cancels for the other. As depicted on Fig 5, to avoid the splitting of the signal energy, a strongly asymmetrical coupler is used with a transmission coefficient close to 1 for one of the 2 signal paths and close zero for the corresponding local path. The second coupler output is discarded. A strong local oscillator input is required to counter act the weak coupler transmission on the local path.

As shown on Fig 5 the Kennedy receiver performs a displacement on the signal constellation in order to null one of the 2 hypotheses on the signal, while doubling the other one. This called an "unconditional nulling receiver". The use of a single photon counter is mandatory when a signal at quantum level is concerned.

Assuming a perfect receiver with a unit quantum efficiency, free of thermal noise and spurious background radiation, no errors occur for the symbol for which the signal field is cancelled by the local oscillator, since no electron may emitted by the vacuum state. When the signal field is doubled by the local oscillator addition, there is a probability lower than unity of emitted photoelectrons since all coherent states overlap with the vacuum state. An error occurs when no photoelectron is emitted when 4Ns are expected. Using again the well-known conditional Poisson process at the photon counter and assuming the same probability for the 2 transmitted symbols, the bit error rate of the Kennedy receiver is obtained

$$BErrorR = 1/2\exp(-4N_s) \tag{26}$$

This is usually referred as the *Super Quantum Limit*[26,27]

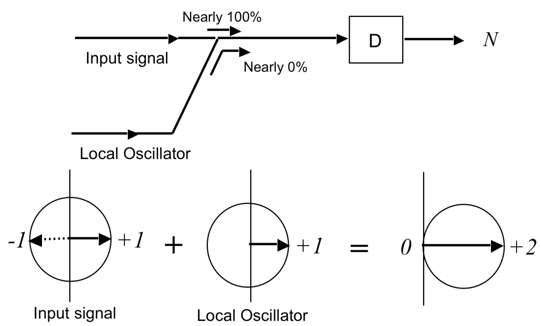

Figure 5: Single detector Kennedy receiver and its Constellation displacement.

The Kennedy receiver does not allow reaching the Helström bound. However this near optimum receiver has a better probability of error for large signal photon number than the "Standard Quantum Limit" (SQL) discussed in Section 5. The photon number required for the probability of error for the Kennedy receiver is twice the photon number that appears in the asymptotic limit $BER = (1/2)\exp(-2N_s)$ of the SQL. This can be understood by considering that, for the 2 detector arrangement achieving the SQL discussed in Section 5, the power of the incoming signal is spread on two detectors and that the 2 detector outputs, proportional to the signal amplitude, are subtracted, recovering a factor 2, while for the Kennedy receiver, the spread signal amplitude is doubled on one detector, and the power therefore squared. In this last case, the signal contribution on the other detector is cancelled.

4.4 Dolinar receiver

Dolinar, also proposed another receiver structure for the binary channel with coherent states using photon counter, in the absence of thermal noise[28,29]. This structure is a "conditional nulling receiver" and is able in principle to reach the Helström bound.

The Dolinar receiver is based on the Kennedy receiver, also with ideal couplers but incorporating an adaptive strategy to implement a feedback whose amplitude can be controlled and its phase switched over the bit duration, in order to dynamically null one hypothesis depending on the observed count process, in a real time feedback scheme. This constitutes a "conditionally nulling" receiver that progressively annuls the more probable signal according to the measured counts. As time goes on the phase is switched less frequently, until a final count after which the input field is almost cancelled. In Dolinar receiver, decision is carried out by the parity of the number of counts at the end of the symbol: hypothesis 1 for odd count and hypothesis 0 for even count. As for the Kennedy receiver the use of a single photon counter is mandatory when signal at quantum level is concerned.

5. DOUBLE DETECTOR OPTICAL RECEIVERS

5.1 Double detector interferometric Kennedy, receiver or double detector super homodyne receiver

The double detector Kennedy receiver or double detector super homodyne receiver is based on the interference of the signal to be detected with a reference one of similar amplitude. The BPSK signal demodulation may be achieved by using a double detector Kennedy receiver so-called double detector super homodyne receiver. A 50% x 50% coupler is used to split the incoming signal on the 2 detectors. The use of photon counters is mandatory when signal at quantum level is concerned. According to its phase, the signal field is cancelled or doubled by the subtraction or the addition of a local field with the same amplitude. This situation is equivalent to an interferometer with a contrast equal to the unity in which a dark fringe occurs on one of the 2 detectors and a bright fringe on the other one.

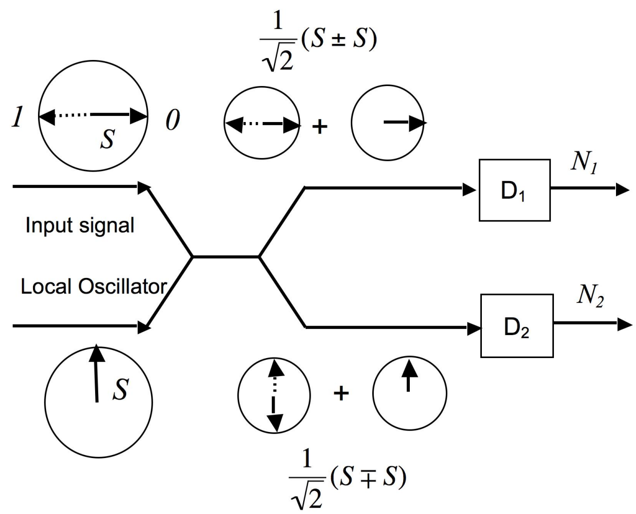

Figure 6: Double detector interferometric Kennedy receiver or double detector super homodyne receiver.

The general double detector super homodyne receiver configuration is depicted on Fig 6. The signal is S, when the symbol 0 is transmitted, and - S, when the symbol 1 is transmitted. So we have

$$a_1 = a_{1I} = s_I = \pm S \quad \text{and} \quad a_2 = ja_{2Q} = jl_I = jS \text{ where } S \text{ is real} \tag{27}$$

In this case Eq.5 is reduced to

$$N_1 = \frac{1}{2}\left(S \pm S\right)^2 = \begin{cases} 2S^2 = 2N_S \text{ when 0 is transmitted} \\ \quad 0 \quad \text{when 0 is transmitted} \end{cases} \tag{28}$$

$$N_2 = \frac{1}{2}\left(S \mp S\right)^2 = \begin{cases} \quad 0 \quad \text{when 0 is transmitted} \\ 2S^2 = 2N_S \text{ when 0 is transmitted} \end{cases} \tag{29}$$

where N_S is the average received signal photon number. This receiver performs an unconditional signal nulling on one of the detectors. In ideal conditions, this receiver produces erasures whatever is the transmitted symbol. An erasure occurs if no photon is received when the expected number is $2N_S$. Using again the well-known probability, for n = 0 and $\langle n \rangle = 2N_S$ as an expected value, we have the theoretical erasure rate

$$BErasureR = \exp(-2N_S) \tag{30}$$

In quantum cryptography applications this arrangement may by used for quantum key distribution. The erasure rate is not usually a major drawback since the corresponding information may be discarded during the reconciliation process at the expense of a reduction of the key rate generation[30,31].

In digital communication the erasures, which are localized, may be easily corrected by using a coding overhead. When no coding is used the erasure rate turns to a *BErrorRate* equal again to the half of the erasure rate

$$BErrorR = 1/2\exp(-2N_S) \tag{31}$$

According to Eq. 3, the average photon number $N_S = 10$ is required to achieve a bit error rate equal to 10^{-9}. Since the signal optical power is split on the 2 detectors and since only a single detector is used at a given time this receiver is equivalent to the Kennedy receiver with only half of the signal energy.

This receiver does not allow to reach the Kennedy receiver sensitivity, because of the prior division to the received field strength signal which is afterward doubled (or cancelled) by the addition of local fields, leading to a signal 3db lower than obtained by doubling the total amplitude of the signal on the single detector Kennedy receiver.

The sensitivity is also obtained by a balanced homodyne detection with a local oscillator of very high amplitude for which a single quadrature of the field is measured. The BER is in this case $BErrorR = 1/2\,\mathrm{erfc}\left(\sqrt{2N_S}\right)$ with the same value asymptote (Standard Quantum Limit).

In a balanced dual detector arrangement the total average bit energy is collected leading to 3db theoretic improvement as compared to the OOK quantum limit. Furthermore input excess noise, as compared to the quantum limit, preserve a strong correlation on the 2 detectors, thanks to the low value of the 2 arm delay and are rejected by the balanced electrical arrangement.

However, as for the Kennedy and the Dolinar receivers, the use of a single photon counter is mandatory when signal at quantum level is concerned.

5.2 Double detector strong local oscillator homodyne receiver for PSK signal

Classical theory of strong local oscillator homodyne detection

The general two-detector PSK coherent receiver configuration is depicted on Fig. 7. The signal is injected in the first port and is S when the symbol 0 is transmitted and $-S$ when 1 the symbol is transmitted. On the second port, a strong local oscillator is assumed to be injected with an amplitude $L >> S$. In this situation we have

$$a_1 = s_I \pm S \quad \text{and} \quad a_2 = -jl_I = -j\mathrm{L} \quad \text{where } S \text{ and } L \text{ are real} \tag{32}$$

In this case Eq.10 is reduced to

$$N = 2s_I l_I = 2SL \tag{33}$$

The detector on which the signal is maximum when the symbol 0 is transmitted is denoted D_1 and the detector on which the signal is maximum when the symbol 1 is transmitted is denoted D_2. Assuming again unit quantum efficiency, the 2 electron counts express as

$$N_1 = \frac{S^2 + L^2}{2} \pm SL = \frac{N_S + N_L}{2} \pm \sqrt{N_S N_L} \tag{34}$$

$$N_2 = \frac{S^2 + L^2}{2} \mp SL = \frac{N_S + N_L}{2} \mp \sqrt{N_S N_L} \tag{35}$$

where N_S and N_L are the average signal and local photon number defined as $N_S = S^2$ and $N_L = L^2$. By subtraction of the two photo detector counts, the final output signal of the receiver is

$$\left|N_2 - N_1\right| = 2\sqrt{N_S N_L} \tag{36}$$

while the output fluctuations are obtained by adding the variances of uncorrelated photon number fluctuations

$$\left\langle(\Delta N\ )^2\right\rangle = \left\langle(\Delta N_0)^2\right\rangle + \left\langle(\Delta N_1)^2\right\rangle = N_L + N_S \approx N_L \tag{37}$$

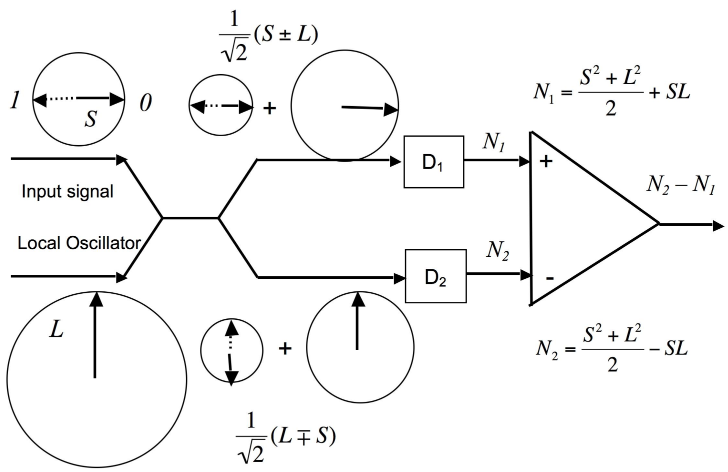

Figure 7: The general two-detector BPSK coherent receiver configuration.

The Poisonian fluctuations of the photon flow from the local oscillator appear here as the dominant noise source. The homodyne detection description is usually done in terms of beating and is therefore closely related to the wave description of light. However, when the output noise is concerned, it is common to switch, as we have done above, to a corpuscular description of the light, leading to the usual conclusion that local-oscillator shot noise, some times thought of as only occurring in photo detection, is the fundamental noise.

The signal to noise ratio is

$$\frac{S}{N} = \frac{N^2}{\left\langle(\Delta N)^2\right\rangle} = \frac{4N_S N_L}{N_L} = 4N_S \tag{38}$$

And the bit error rate is

$$BErrorR = 1/2\,\mathrm{erfc}\left(\sqrt{2N}_S\right) \tag{39}$$

which is referred as the “Standard Quantum Limit”, with the asymptotic value

$$BErrorR = 1/2\exp\left(-2N_S\right) \tag{40}$$

According to Eq.40 an average photon number N_S = 9 is required to achieve a bit error rate equal to 10^{-9}. In this case, only a single quadrature of the signal field is observed. This result is the same as for the double detector Kennedy receiver, but, thanks to the noise free mixing gain, this receiver allows the utilization of standard PIN photodiode and avoids the photon counters impairments.

It is to be noticed that for a PSK signal demodulation with an heterodyne arrangement, an average photon number N_S = 18 photons would be required to achieve a bit error rate equal to 10^{-9}, due to the 3dB penalty of the simultaneous measurement of the 2 quadratures of the local field. Homodyne detection of an OOK modulated signal would require also N_S = 18 photons since no signal would be transmitted half of the time. Heterodyne of an OOK modulated signal would require N_S = 36 photons, due to the 3dB penalty of the simultaneous measurement 2 quadratures.

Quantum theory of strong local oscillator homodyne detection

The quantum theory of the homodyne detection has already been widely discussed[32,33,34,35]. In homodyne detection only one quadrature is measured and no noise addition is required. The input signal quantum noise is therefore the only noise limitation. The local oscillator has no influence and the output noise is only governed by vacuum fluctuation entering at the signal port. The coherent subtraction of the 2 photocurrents outputs allows also homodyne detection to reject the classical and the quantum fluctuations of the oscillator local as well. As a consequence, homodyne detection is only limited by the quantum fluctuation of the signal, i.e. the vacuum fluctuation entering through the signal port.

The local oscillator shot noise is produced by the vacuum fluctuation, entering through the local port. It has no influence on the output noise. However it may be considered in a naïve description of the classical theory, with valid numerical results.

5.3 Comparison of strong local oscillator and super homodyne receiver for PSK signal

The Table 1 compares the super homodyne receiver using the photon counters strong reference balanced homodyne receiver using PIN photodiodes.

Super Homodyne Receiver with Photon Counters	**Strong Reference Balanced Homodyne Receiver with PIN Photodiodes**
Photon counter (gated Geiger APD) - Low speed (MHz) - Low quantum efficiency (10%) - Dark count limit (QBER) - Cooling required - Quenching required	Standard PIN photodiode - High speed (GHz) - High quantum efficiency (90%) - Room Temperature - Low cost
No strong reference (local oscillator) requirement Interferometric arrangement may be use	Strong reference (local oscillator) requirement Noise free mixing gain
Decision threshold - At the counter level - Trade-off between efficiency and dark count	Decision threshold - Post detection at high signal level - Multi level decision possible
Erasure rate at twice the Standard Quantum Limit (SQL) BER	Standard Quantum Limit (SQL) BER

Table 1: Comparison of the 2 double detector receivers for PSK signal

5.4 Comparison of the different coherent PSK receivers implementation and performances

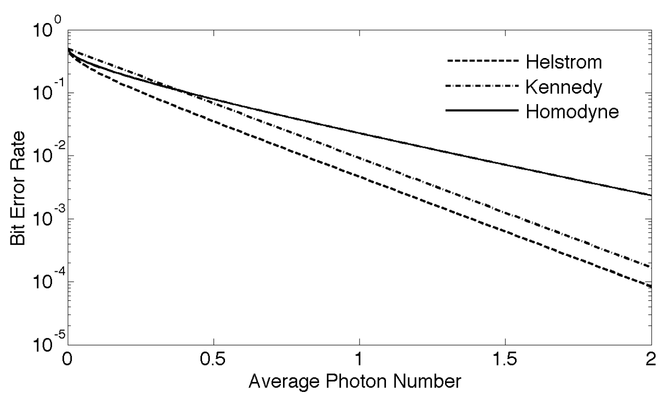

Figure 8: Bit error rate obtained with the strong oscillator homodyne detection arrangement, at the Helström limit and with the single detector Kennedy receiver, in terms of the signal energy.

The Fig.8 compares, in terms of the signal energies, the bit error rate of the strong oscillator homodyne detection arrangement to the Helström limit and to the single detector Kennedy receiver performances

The Table 2 summarizes the different receiver implementations and their performances expressed in term of bit error rate.

Quantum receiver	**Bit Error Rate**	**Asymptotic approximation**	**Implementation requirement**	**Comments**
Helström limit Dolinar receiver	$1/2\left(1-\sqrt{1-\exp(-4N_S)}\right)$	$1/4\exp(-4N_S)$	Idealist combiner Single Photon Counter	Conditional nulling Phase et amplitude feed-back control
Super homodyne Kennedy receiver	$1/2\exp(-4N_S)$	$1/2\exp(-4N_S)$ Super Quantum Limit	Realistic Balance Mixer Single Photon Counter	Unconditional nulling receiver Thermal noise limitation
Homodyne detection	$1/2\,\mathrm{erfc}\left(\sqrt{2N_S}\right)$	$1/2\exp(-2N_S)$ Standard Quantum Limit	2 PIN photodiodes	Quantum Limit Mixing gain overcoming thermal noise
Heterodyne detection	$1/2\,\mathrm{erfc}\left(\sqrt{N_S}\right)$	$1/2\exp(-N_S)$	2 PIN photodiodes	Free running local oscillator
Direct detection of OOK signals	$1/2\exp(-2N_S)$ Standard Quantum Limit	$1/2\exp(-2N_S)$ Standard Quantum Limit	Single PIN thermal noise free photodiode	Usually impaired by thermal noise

Table 2: Comparison of the different receivers implementations and performances expressed in term of bit error rate

6. TWO EXPERIMENTS WITH BALANCED HOMODYNE DETECTION

Up to now we have elaborated on the balanced homodyne detection technique for applications employing phase shift keying, we obtained its performances in terms of signal to noise ratio and bit error rate and compared both with the fundamental bounds and with the performance of heuristic receivers based on photon counting. We will finally illustrate experimentally the operation and measured performance of this type of detection, for the PSK-modulated optical channel.

In this section we present two experimental set ups for the balanced homodyne detection of weak coherent state fields, both operating at the telecommunications wavelength 1550 nm: one in continuous wave and the other in pulsed regime. They are intended for quantum key distribution applications, comprising also conjugated base switching at transmitter and receiver ends, however for our present task we will concentrate only on the production of the weak coherent PSK signal and the local oscillator, as well as the field mixing and balanced homodyne detection.

Both set ups are based on interferometric self-homodyne configurations, which substantially relaxes the postdetection processing, since the strong cross-correlation between the signal and the local oscillator fields yields a very narrowband post detection process at baseband, and only slow interferometric drifts need to be compensated.

6.1 Continuous wave balanced homodyne detection

Our first experiment uses both signal and local oscillator in continuous wave regime. In fact they travel in separate fibers are recombined at the receiver end. Even in the self-homodyne configuration the interferometer must be precisely stabilized in the presence of perturbations, which we perform by applying phase synchronization techniques.

For power economy we employ suppressed carrier PSK, i.e. no residual carrier to lock to. Therefore we need to access both field quadratures in order to provide the phase error for the synchronization; however balanced homodyne detectors measure only one signal quadrature, i.e. that orthogonal to the local oscillator phasor. Diverse synchronization techniques have been proposed using time-switching phase diversity both for the classical channel[36,37,38] as well as the quantum channel[39]; in this work we propose a detection structure based on sequential I-Q detection, using a switched-phase local oscillator.

We have implemented an experimental system with a balanced homodyne scheme employing a continuous wave light source at 1550 nm wavelength. Fig 9 is a simplified scheme of our experimental set up (polarization control elements are not shown).

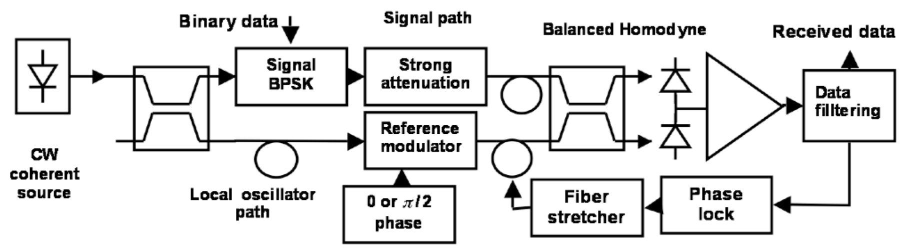

Figure 9: Continuous wave experimental set up with separated fibers for signal and local oscillator

In order to separate problems related to finite laser line width when using a separate local oscillator our set up uses the same laser source for the signal and local oscillator, which is obtained by splitting the laser source. The transmitted signal is phase modulated and strongly attenuated in order to produce a weak coherent state field and sent through a standard telecommunications fiber. The local oscillator travels in a separate fiber.

At the receiver end the weak signal and the strong local oscillator are detected in a balanced homodyne configuration. In order to generate the phase error, i.e. remove the modulation we need to process non-linearly the in-phase and quadrature components. This is performed with a scheme that alternatively switches the local oscillator phase between 0◦ and 90◦to sequentially beat with the signal. Phase error is finally feedback into an optoelectronic loop acting on a fiber stretcher to precisely equalize the path lengths.

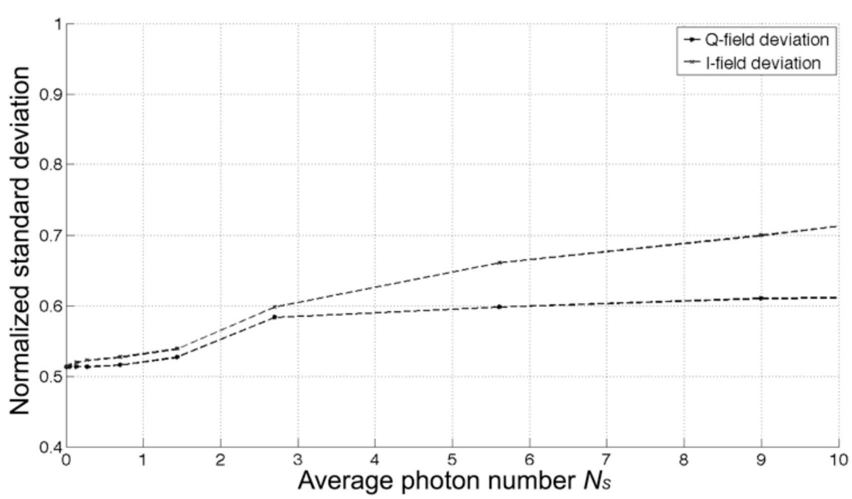

Figure 10: Measured uncertainty product for the continuous wave balanced homodyne experiment.

Fig. 10 shows our experimental results on for the uncertainty product as a function of signal photon number, our measurements are close to the uncertainty limit[40,41], especially for small values of the photon number. These results are interpreted as that the attenuation of optical signal power smoothes out the excess noise and the strongly attenuated signal approaches the coherent states model.

6.2 Pulsed source balanced homodyne detection

Our second experimental set up is based also on a balanced homodyne scheme, but employing a pulsed light source at 1550 nm wavelength, in a multiplexed scheme that has the advantage of requiring only one fiber for the communication channel. Fig.11 is a simplified scheme of our experimental set up (polarization control elements are not shown).

In order to isolate the above mentioned problems related to finite laser line width when using a separate local oscillator, this time our set up uses time multiplexed signal and local oscillator in the optical channel, which is obtained by splitting the laser field in an interferometric scheme, with a delay in one arm for the (strong) local oscillator laser pulse.

In the other arm the transmitted signal is phase modulated either by the information or by training frames (see below) for phase lock purposes at the receiver end. We strongly attenuate the transmitted signal in order to produce a weak coherent state field and send it through a standard telecommunications fiber.

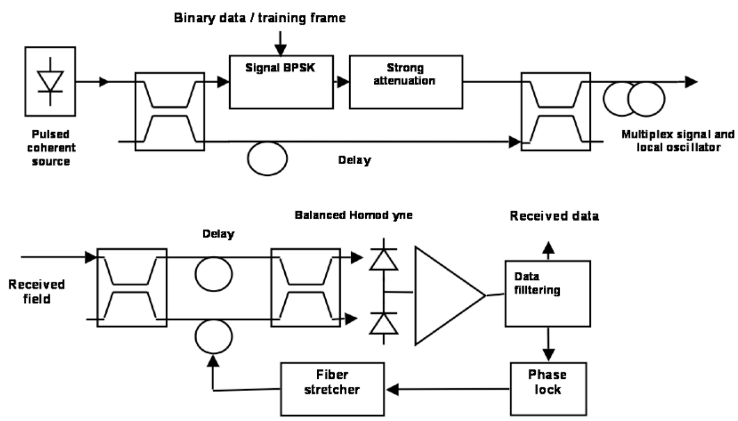

Figure 11: Set up for the balanced homodyne detection experiment with pulsed source: upper part: transmitter; lower part: receiver.

At the receiver end the weak signal and the strong local oscillator pulses are superimposed in a similar interferometric scheme using the same delay, and a balanced homodyne configuration is used for detection. Even in this multiplexed scheme we still have to deal with the optical phase synchronization problem due to the effects of both interferometers at the transmitter and the receiver. Diverse synchronization techniques have been proposed using synchronization bits both for classical telecommunications channels[42], low photon-number interferometry[43], as well as in quantum cryptography[44].

In this work the phase drift is compensated with an optoelectronic feedback using training frames inserted at regular intervals at the transmitter as shown on Fig 11. At the receiver we extract this information from the postdetection signal to generate an error signal that is used for acting on a fiber stretcher.

Fig.12 shows our experimental results for the BER as a function of signal photon number, compared to the standard quantum limit.

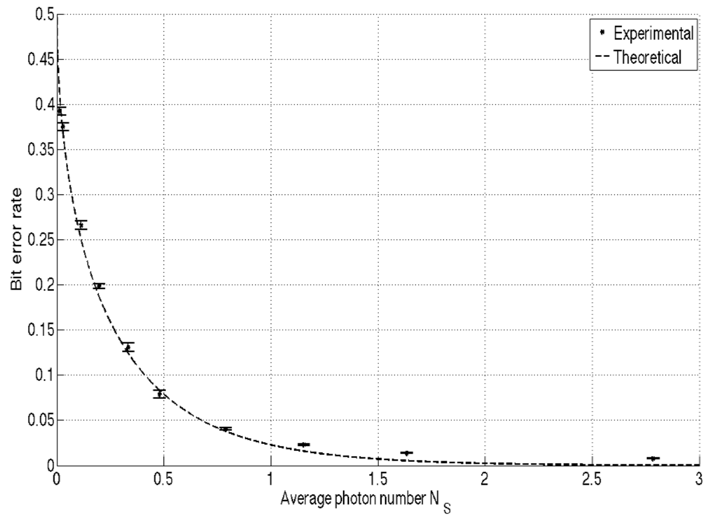

Figure 12: Experimental results for the BER as a function of signal photon number

7. CONCLUSION

We have presented basic concepts related to optical signals and quantum noise and its repercussion on the transmission of information: quantum noise becomes the ultimate limitation when thermal noise is surmounted by employing suitable detection systems, such as cooled photon counters or room temperature heterodyne and homodyne detectors with strong reference fields. The manifestation of quantum phenomena sets the fundamental bounds in the minimum energy per bit, which are of great interest in present and new applications that operate with few photons per observation time such as quantum communications and cryptography, either for power economy or for quantum state preparation requirements.

We focused on the quantum coherent state model of the radiation field, as they most closely resemble the classical description, and many concepts are understandable from this representation, as a result of commutation and uncertainty relations. However, they are non-orthogonal and a finite error rate is unavoidable: we presented the fundamental detection bounds and some receiver structures that approach those bounds.

In this work we emphasized on the homodyne detection, which has been extensively developed for classical systems, due to its interesting characteristics concerning noise free conversion gain to approach the standard quantum limit, using standard PIN photodetectors. These characteristics are also attractive in other applications such as free space communications, lidar, radio over fiber, optical sensors, and other sensitive to power economy.

Traditional models for homodyne detection interpreted noise as produced by the local oscillator shot noise. However in recent applications a more detailed description is necessary, we therefore presented a quantum treatment explaining the fact that the noise in balanced homodyne detection (as well as in heterodyne) is due to quantum fluctuations at the signal port. Since a single quadrature is measured, this detection is limited by the uncertainty principle with no additional noise required.

We thus elaborate on this detection technique for applications employing phase shift keying, obtaining the performances in terms of signal to noise ratio and bit error rate and comparing both with the fundamental bounds and with the performance of heuristic receivers based on photon counting.

Finally we experimentally illustrated the operation and performance of balanced homodyne detection, at the telecommunications wavelength, employing weak coherent states, presenting two experimental set ups: continuous wave and pulsed PSK-modulated; we measured their performances in uncertainty product and bit error rate and compared with the standard quantum limits.

REFERENCES

[1] Bennett C. H., 1984, and G. Brassard, Quantum cryptography: public key distribution and coin tossing, Proceedings of the International Conference on Computer Systems and Signal Processing, Institute of Electrical and Electronics Engineers, New York, pp. 175-179.

[2] Gisin N., 2002, G. Ribordy, W. Tittel, and H. Zbinden, Quantum cryptography, Rev. Mod. Phys. 74, 145-195.

[3] Scarani, V., Bechmann-Pasquinucci, H., Cerf, N.J., Dusek, M., Lutkenhaus, N., Peev, M. (2009), The Security of Practical Quantum Key Distribution, Reviews of Modern Physics, Vol. 81, pp. 1301-1350.

[4] Mérolla J.M., 1999a, Y. Mazurenko, J.P. Goedgebuer, H. Porte and W. T. Rhodes, Phase-modulation transmission system for quantum cryptography, Opt. Lett., 24, pp. 104-106.

[5] Xu Q., Arvizu A., Gallion P. And Mendieta F.J.. Homodyne In-Phase and Quadrature Detection of Weak Coherent States with Carrier Phase Tracking. IEEE Journal of Selected Topics in Quantum Electronics, IEEE Volume 15, Issue 6, Page(s): 1581 - 1590, Nov.-dec. 2009

[6] Xu Q., Costa E Silva M.B., Sabban M., Gallion P. And Mendieta F.J., Dual-Threshold Balanced Homodyne Detection at 1550nm Optical Fiber Quantum Key Distribution System,. IEEE/OSA Journal of Lightwave Technology

[7] Toyoshima M. et al. (2008), "Free – space quantum cryptography with quantum and telecom communication channels", Acta Astronautica, 63, pp. 179-184

[8] Riguidel, M., (2005), "Quantum Crypt: Enhancement of AGT Communications Security Using Quantum Cryptography", Report ENST/EEC/QC.12.01.WP3.A, http://www.infres.enst.fr/~bellot/publis/wp3.pdf

[9] Villoresi, P. et al, (2008) "Experimental verification of the feasibility of a quantum channel between Space and Earth", New J. Phys. 10, 033038

[10] Chan, V.W.S., (2006)"Free space optical communications", IEEE Journal of Lightwave Technology, Vol. 24, No. 12, pp. 4750-4762.

[11] Miao, E.L. et al., "The feasibility of geostationary satellite –to – ground quantum key distribution", Physics Letters A, 361, pp. 29-32 (2007)

[12] Villoresi, P. et al, Space-to-ground quantum-communication using an optical ground station: a feasibility study Proc. of SPIE Vol. 5551, 113-120 (2004), Quantum Communications and Quantum Imaging II, R. Meyers and Y. Shih (eds.) [quant-ph/0408067]

[13] Ursin R. et al., "Space QUEST Experiments with quantum entanglement in space", IAC Microgravity Sciences and Processes Symposim, Glasgow, Scotland, 2008.

[14] Pfenningbauer, M. et al., 2005, « Satellite – based quantum communication terminal employing state – of – the – art technology", OSA Journal of Optical Networking, Vol. 4, no. 9, pp. 549-560

[15] Aspelmeyer, M. et al, "Long-Distance Quantum Communication with Entangled Photons using Satellites", IEEE Journal of Selected Topics in Quantum Electronics, special issue on "Quantum Internet Technologies", Vol. 9, 1541-1551 (2003) [quant-ph/0305105]

[16] Kaltenbaek, R. et al, "Proof-of-Concept Experiments for Quantum Physics in Space", Proc. of SPIE Vol. 5161, 252-268 (2003), Quantum Communications and Quantum Imaging, R. Meyers and Y. Shih (eds.) [quant-ph/0308174].

[17] Pulford, D., (2005), "Single photon locking of an all-fiber interferometer", Review of Scientific Instruments, Vol. 76, No. 6, pp. 063114-1-5.

[18] Zavatta, A., et al,(2002), « Time domain analysis of quantum states of light: noise characterization and homodyne tomography », J. Opt. Soc. Am. B, Vol. 19, No. 5, pp.1189-1194.

[19] McKenzie K. et al, (2005), "Quantum Noise Locking", J. Opt. B: Quantum Semiclass. Opt. Vol. 7, pp. 5421-5428.

[20] Helstrom C.W., 1976, Quantum Detection and Estimation Theory, Academic Press, New York.

[21] Gallion P., Mendieta F.J. And Jiang S., Signal and quantum noise in optical communication and in cryptography. Elsevier 2008, Progress in Optics, Volume 52, Jan 2009.

[22] Haus H.A., 1995, Frederic Ives Medal Paper, From classical to quantum noise, J. Opt. Soc.Am. B, 12, 11, 2019-2036..

[23] Gallion P., 2002, Basics of Digital Optical Communications, Undersea Fiber Systems, J. Chesnoy, pp. 51-93, Academic Press, New York.

[24] Kennedy R.S., 1973, A near-optimum receiver for the binary coherent state quantum channel, Quarterly Progress report No. 108, Research Laboratory of Electronics, MIT, pp. 219-225.
[25] Yuen H.P., 1970, R.S Kennedy and M. Lax, On optimal quantum receivers for digital signal detection, Proceedings IEEE, 58, pp. 1170-1173.
[26] Saltz J., 1986, Modulation and detection for coherent lightwave communications, IEEE Communications Magazine, 24, pp 38-49.
[27] Salz, J., 1985, Coherent lightwave communications, AT&T Tech. J., vol.10, pp 2153-2209.
[28] Dolinar S., 1973, An optimum receiver for the binary coherent state quantum channel, Quarterly Progress report No. 111, Research Laboratory of Electronics, MIT, pp. 115-120.
[29] Lau C.W., 2006, V.A. Vilnrotter, S. Dolinar, J.M. Geremia and H. Mabuchi Binary quantum receiver concept demonstration, Proc. SPIE Free Space Laser Communication Technologies XVIII, Vol. 6105, 61050J1-7.
[30] Hirano T., 2003, H. Yamanaka, M. Ashikaga, T. Konishi and R. Namiki, Quantum cryptography using pulsed homodyne detection, Phys. Rev. Lett, A 68, 042331-1-042331-7..
[31] Xu Q., Sabban M. and Gallion P., Homodyne Detection of Weak Coherent Optical Pulse with Selection of Decision Opportunity: Applications to Quantum Cryptography. Microwave and Optical Technology Letters Volume 51, Issue8, pp1934-1939.
[32] Yuen H.P., 1983, and V.W.S. Chan, Noise in homodyne and heterodyne detection, Opt. Lett., 8, pp. 177-179
[33] Schumaker, B.L., 1982, Noise in homodyne detection, Opt. Lett., 9, pp. 189-191.
[34] Ban M., 1997, Quantum theory of the homodyne-direct receiver, Journal of Modern Optics, Vol. 44, No. 6, pp. 1175-1195.
[35] Shapiro J.H., 2003, Quantum Gaussian noise, Proceedings of SPIE Vol.5111, Fluctuations and Noise in Photonics and Quantum Optics, Derek Abbott, Jeffrey H. Shapiro, Yoshihisa Yamamoto, Editors, pp. 382-395.
[36] Glatt, W., Schreiblehner, M.A., Haider, C. and Lebb, W.R., "Optical PSK homodyne system using a switched residual carrier for phase synchronization", Electronics Letters, Vol. 32, No. 15, pp. 1386-1387 (1996).
[37] Fabrega J. M. and Prat, J., “Homodyne receiver prototype with time-switching phase diversity and feedforward analog processing”, Optics Letters, Vol. 32, No. 5, pp. 463-465 (2007).
[38] Habbab, L.M.I., Kahn, J.M. and Greenstein, J.I., “Phase insensitive zero I.F. coherent optical system using phase switching”, Electron. Lett. Vol. 24, No. 5, pp. 974-976 (1988).
[39] Koashi, M., “Unconditional security of coherent state quantum key distribution with a strong reference phase pulse,” Phys. Rev. Lett., vol. 93, p. 120501 (2004).
[40] Opatrny, T., Dakna, M. and Welsch, D. G., “Number-phase uncertainty relations: verification by balanced homodyne measurement,” Phys. Rev. A, vol. 57, pp. 2129–2133, (1998).
[41] Smithey, D.T., Beck, M., Cooper, J. and Raymer, M. G., “Measurement of number-phase uncertainties of optical fields,” Phys. Rev., vol. A48, pp. 3159–3167 (1993).
[42] Wandernoth, B., "20 photons/bit 565 Mbit/s PSK homodyne receiver using synchronization bits", Electronics Letters, Vol. 28, No. 4, pp. 387-388 (1992).
[43] Makarov, V., Brylevski, A. and Hjelme, D. R., “Real-time phase tracking in single-photon interferometers”, J. Appl. Opt. 43, pp. 4385–4392 (2004).
[44] Elliott, B.B., Pikalo, O., Schlafer, J. and Troxel, G., “Path-length control in an interferometric QKD link”, Quantum Information and Computation, Proceedings of the SPIE, 5105, pp. 26-38 (2003).